Energy Transfer Mediated Fluorescence from Blended Conjugated Polymer Nanoparticles

Changfeng Wu, Hongshang Peng,† Yunfei Jiang, and Jason McNeill*

Department of Chemistry and Center for Optical Materials Science and Engineering Technologies, Clemson University, Clemson, South Carolina 29634

Received: March 23, 2006; In Final Form: May 19, 2006

Nanoparticles consisting of a derivative of the blue-emitting conjugated polymer polyfluorene doped with green-, yellow-, and red-emitting conjugated polymers were prepared by a reprecipitation method. The nanoparticles can be described as a system of densely packed chromophores that exhibit efficient energy transfer from the host to the dopant polymers. Fluorescence quenching analysis of the host polymer as a function of the dopant concentration indicates that one energy acceptor molecule can effectively quench 90% of the fluorescence of a nanoparticle consisting of 100−200 host conjugated polymer molecules. A nanoparticle energy transfer model was developed that successfully describes the quenching behavior of a small number of highly efficient energy acceptors per nanoparticle. The fluorescence brightness of the blended polymer nanoparticles was determined to be much higher than that of inorganic quantum dots and dye-loaded silica particles of similar dimensions. The combination of high fluorescence brightness and tunable fluorescence of these blended nanoparticles is promising for ultrasensitive fluorescence-based assays.

1. Introduction

Highly fluorescent nanoparticles have attracted much attention due to a variety of fluorescence-based applications such as biosensing, imaging, and high-throughput assays.[1−4] Inorganic semiconductor quantum dots and dye-loaded beads are currently employed in a number of demanding fluorescence applications such as live cell imaging.[5−9] Conjugated polymers are known to possess high absorption coefficients and high fluorescence efficiency, which have led to a wide range of applications in optoelectronic thin film devices.[10−13] Ultrasensitive sensing schemes based on superquenching of water-soluble conjugated polyelectrolyte fluorescence in aqueous solution have also been demonstrated.[14−19] However, the use of conjugated polymer *nanoparticles* in fluorescence labeling is still a largely unexplored area. For the biological applications such as in vivo sensing and imaging, the nanoparticles must be soluble, stable, relatively free of nonspecific interactions,[20] and sufficiently bright in aqueous dispersions. We have recently developed a simple method for obtaining highly fluorescent nanoparticles that consist primarily of single conjugated polymer molecules.[21,22] Particle morphology was characterized by AFM and TEM, while the optical cross-sections of individual particles were probed by using near-field scanning optical microscopy. Encapsulation and amine functionalization of the nanoparticles were also demonstrated.

While interest in the photophysics of doped or disordered systems of densely packed chromophores spans several decades,[23−26] recent interest in emerging applications such as nanophotonics[27,28] and single-photon sources[29,30] has caused a resurgence of interest in such systems. Single conjugated polymer molecules[31−33] and conjugated polymer aggregates[34,35] exhibit complex photophysics and surprising phenomena such as blinking and photon antibunching,[30] which are attributable to a variety of processes that occur in such complex systems. Energy transfer in nanoscale systems has recently been demonstrated as the basis of molecular beacons for efficient biomolecule detection.[36−38] Our understanding of the photophysics of such systems is currently limited by the lack of experimental results on well-behaved model systems and by difficulties in interpreting their behavior. Nanoparticles and nanoparticle assemblies are typically heterogeneous systems. Analysis of energy transfer in nanoparticles of mixed composition or in donor−acceptor nanoparticle assemblies is complicated by the fact that, in many cases, there are a small number of quenchers per molecule, resulting in a statistical distribution of energy acceptors and significant particle-to-particle variations in quenching efficiency. In such systems, there can be significant deviations from Stern−Volmer quenching theory.[15,16,39]

Here we report on energy transfer mediated fluorescence from conjugated polymer nanoparticles consisting of polyfluorene (PF) doped with three different conjugated polymer acceptors. The blended conjugated polymer nanoparticles exhibit fluorescence excitation spectra characteristic of the host polymer, and the fluorescence emission spectra characteristic of the dopant polymer. Stern−Volmer analysis of the host fluorescence as a function of dopant concentration indicates efficient energy transfer from a hundred or more host polymer molecules to a *single* dopant polymer molecule. These blended nanoparticles are many times brighter than inorganic quantum dots and dye-loaded silica particles of similar dimensions—in one case, a nanoparticle fluorescence quantum yield of 14% and a peak extinction coefficient of 1.5×10^9 M^{-1} cm^{-1} were determined. The tunable fluorescence properties and high brightness of these nanoparticles are promising for fluorescence-based imaging and sensing applications. Additionally, these particles serve as a model system for energy transfer in complex nanoscale systems consisting of densely packed chromophores. We present an energy transfer model that yields population-averaged quenching efficiencies for the case of a statistical distribution of a small number of highly efficient energy acceptors per nanoparticle.

* To whom correspondence should be addressed. E-mail: mcneill@clemson.edu.

† Present address: Institute of Optoelectronic Technology, Beijing Jiaotong University, Beijing 100044, China.

10.1021/jp0618126 CCC: $33.50
Published on Web 06/30/2006

For the doped conjugated polymer nanoparticles, the model successfully reproduces the observed dependence of quenching efficiency on average particle composition over a wide range.

2. Experimental Section

2.1. Materials. The conjugated polymer polyfluorene derivative poly(9,9-dihexylfluorenyl-2,7-diyl) (PF, MW 55 000, polydispersity 2.7), the copolymer poly[{9,9-dioctyl-2,7-divinylenefluorenylene}-*alt*-*co*-{2-methoxy-5-(2-ethylhexyloxy)-1,4-phenylene}] (PFPV, MW 270 000, polydispersity 2.7), poly[(9,9-dioctylfluorenyl-2,7-diyl)-*co*-(1,4-benzo-{2,1′,3}-thiadiazole)] (PFBT, MW 10 000, polydispersity 1.7), and the polyphenylenevinylene derivative poly[2-methoxy-5-(2-ethylhexyloxy)-1,4-phenylenevinylene] (MEH−PPV, MW 200 000, polydispersity 7.0) were purchased from ADS dyes. Tetrahydrofuran (THF, anhydrous, 99.9%), was purchased from Aldrich. All chemicals were used without further purification.

2.2. Nanoparticle Preparation. Preparation of the aqueous dispersion of blended conjugated polymer nanoparticles is performed by using a method similar to the reprecipitation method described previously.[21,22] First, dilute solutions of PF (host) and PFPV, PFBT, and MEH−PPV (dopants) were prepared as follows. The polymer was dissolved by stirring overnight in THF under inert atmosphere. The solution was then filtered through a 1.6 μm filter and further diluted to a concentration of 40 ppm. In our previous reports, a lower concentration of conjugated polymer was employed, resulting in smaller particles (∼10 nm in diameter),[21] while the higher concentrations employed here result in larger particles (20−30 nm in diameter). Varying amounts of a dopant polymer solution were mixed with a solution of host polymer to produce solution mixtures with a constant host concentration of 40 ppm and dopant/host fractions ranging from 0 to 10 wt %. The mixtures were stirred to form homogeneous solutions. A 2 mL quantity of the solution mixture was added quickly to 8 mL of deionized water while sonicating the mixture. The resulting suspension was filtered with a 0.2 μm membrane filter. The THF was removed by partial vacuum evaporation, followed by filtration through a 0.2 μm filter. The resulting nanoparticle dispersions are clear and stable for months with no signs of aggregation.

2.3. Characterization Methods. Morphology and size distribution of the polymer blend nanoparticles were characterized by atomic force microscopy (AFM). For the AFM measurements, one drop of the nanoparticle dispersion was placed on an oxidized silicon wafer. After evaporation of the water, the surface was scanned with a Digital Instruments multimode AFM in tapping mode. Olympus cantilevers, with a spring constant of 42 N/m, resonating at 300 kHz, have been used for all measurements. The UV−vis absorption spectra were recorded with a Shimadzu UV-2101PC scanning spectrophotometer, using 1 cm quartz cuvettes. Fluorescence spectra were collected with a commercial fluorometer (Quantamaster, PTI, Inc.), using a 1 cm quartz cuvette.

3. Results and Discussion

3.1. Nanoparticle Size and Morphology. We recently developed a facile method to produce aqueous nanoparticle dispersions of a variety of hydrophobic conjugated polymers.[21,22] The preparation involves rapid addition of a polymer solution (prepared with a water-miscible organic solvent) to water. Figure 1a presents the chemical structures of the conjugated polymers employed in this study. PF was chosen as the host polymer in view of its high absorptivity in the near-ultraviolet region and favorable spectral overlap with the dopant polymers employed in this study. Polymer blend nanoparticles were obtained by quickly adding a solution mixture to water under simultaneous sonication to improve mixing. After removal of a small fraction of aggregates by filtration and removal of THF by partial vacuum evaporation, the composition of the resulting dispersion is consistent with the relative amounts of PF and dopant in the precursor solution mixture, as determined by UV−vis absorption spectroscopy. The nanoparticle dispersions were drop-cast onto silicon substrates for analysis of particle size and morphology by tapping-mode AFM. A representative AFM image of polymer blend nanoparticles is shown in Figure 1b. A particle height histogram obtained from the AFM image indicates that most particles possess diameters in the range of 20−30 nm, as shown in Figure 1c. The lateral dimensions are also in the range of 20−30 nm after the tip width is taken into account.[40] The morphology is consistent with the recent observation that the equilibrium shape for small sized PF nanoparticles (<30 nm) tends to be spherical because surface tension effects determine the morphology in this size range.[41] There are an estimated 100−200 polymer molecules per nanoparticle, assuming densely packed spherical particles. The presence of dopant has no apparent effect on particle size and morphology.

3.2. Optical Properties. Energy transfer in conjugated polymer blends has recently been demonstrated as a viable strategy for improving the quantum efficiency and tuning the emission color of optoelectronic devices.[42−45] However, segregation of the polymer species frequently occurs, causing low energy transfer efficiency. Unlike previously reported methods of producing blended conjugated polymer nanostructures,[46,47] in which there is spectroscopic evidence of polymer segregation, the nanoparticles reported here are produced by a rapid mixing process that apparently reduces the degree of segregation, as evidenced by the efficient energy transfer from the host to guest molecules and the lack of dopant aggregate features in the spectrum. Figure 1d illustrates the evolution of the fluorescence color as the dopant species is varied for aqueous suspensions of nanoparticles under UV lamp excitation (365 nm). At a dopant fraction of 6 wt %, the fluorescence from PF is almost completely quenched and the blend nanoparticles present strong fluorescence from the dopant species. This result indicates highly efficient energy transfer from the host to dopant polymers. Fluorescence spectroscopy and energy transfer phenomena in these blend nanoparticles are discussed in detail below.

The left side of Figure 2 presents the normalized absorption and fluorescence emission spectra of the conjugated polymers PF, PFPV, PFBT, and MEH−PPV in THF solutions. PF, PFPV, PFBT, and MEH−PPV exhibit their peak fluorescence at around 415, 500, 535, and 550 nm, respectively. Conjugated polymers typically have a small Stokes shift between absorption and fluorescence, similar to that of many organic fluorescent dyes, though the combined effects of energetic disorder, energy transfer, and the presence of aggregate species can lead to larger shifts.[48,49] The pure PF nanoparticles (Figure 2, right) show a broadened and blue-shifted absorption as compared to that of the PF in THF solution, which is consistent with an overall decrease in the conjugation length induced by bending or kinking of the polymer backbone.[50] The fluorescence spectrum of the PF nanoparticles (Figure 2, right) is red-shifted by 15 nm relative to that of PF in THF solution. Since the nanoparticles possess a compact structure, the red-shift in fluorescence can be attributed to increased interchain interactions, leading to energy transfer to low-energy chromophores and weakly fluorescent aggregates.[21] The fluorescence emission spectrum of the nanoparticles also has a long red tail, consistent with the

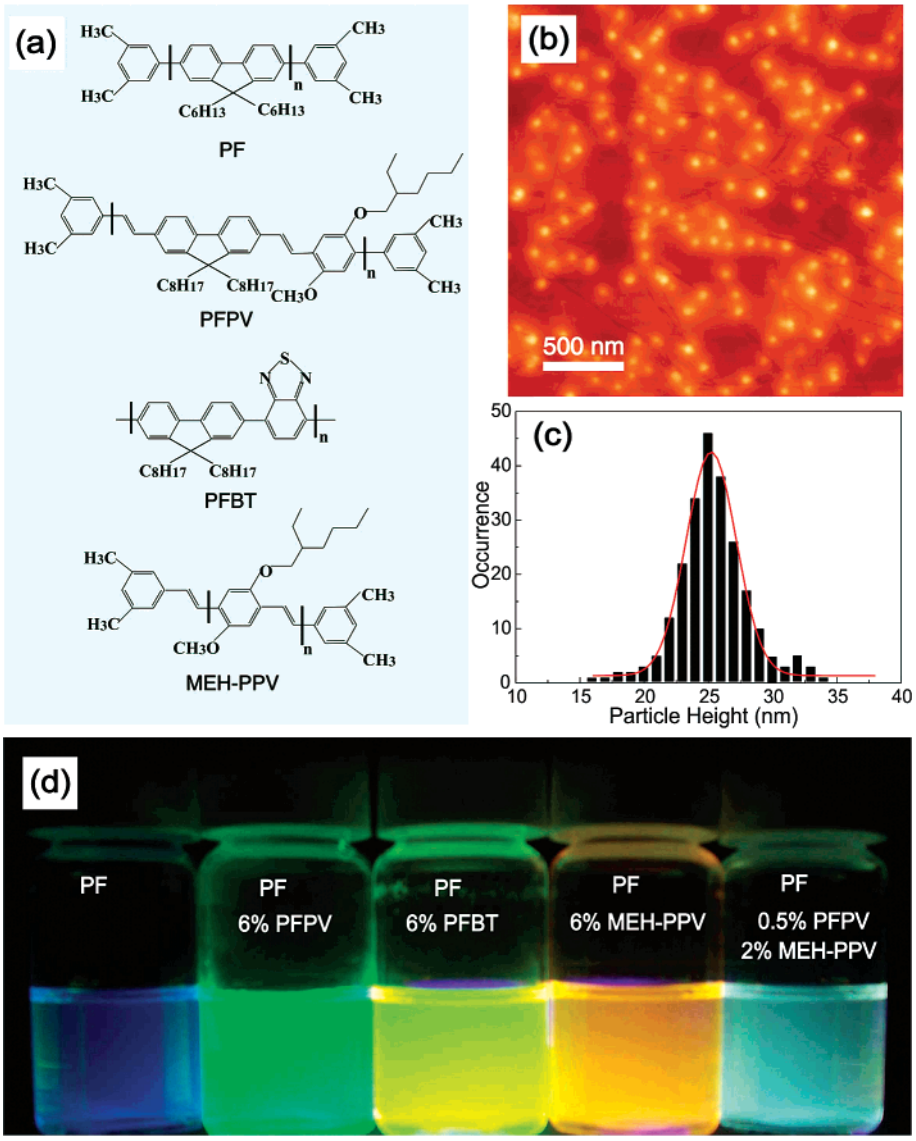

Figure 1. (a) Chemical structures of the conjugated polymers; (b) a representative AFM image of blend nanoparticles dispersed on silicon substrate (measured at a setpoint of 1.68 V); (c) histogram of particle height data taken from AFM image; and (d) photograph of fluorescence emission from aqueous suspensions of the blend nanoparticles taken under a UV lamp (365 nm). The composition of these nanoparticles is indicated on the vials.

presence of aggregate species. Similar features are observed in the fluorescence emission spectra of PF thin films.[51,52] The fluorescence of the host polymer PF in the 400−450 nm range possesses good overlap with the absorption spectra of the three dopant polymers, as required for efficient energy transfer via the Förster mechanism.

The right side of Figure 2 shows the normalized absorption (dashed curves) and fluorescence excitation and emission spectra (solid curves) of the pure PF and three different polymer blend nanoparticles containing 6 wt % dopant PFPV, PFBT, and MEH−PPV, respectively. The dominant absorption peaks (around 375 nm) of the blend nanoparticles are consistent with PF, while the weak absorption peaks in the 400−500 nm range originate from the dopant polymers. With 375 nm excitation, where >95% of the absorption is due to PF, the fluorescence from PF is almost completely quenched, and the nanoparticles exhibit fluorescence emission spectra characteristic of the dopant species. Fluorescence excitation spectra (obtained with the collection wavelength set to match the dopant emission) are very similar to the normalized absorption spectra of PF (with minor differences attributable to the spectrum of the Xe lamp of the fluorometer). These observations indicate efficient intraparticle energy transfer from the PF host to the dopant polymer and are consistent with a low degree of segregation of the dopant polymer. For comparison, the mixed THF solutions of PF and dopant polymers with the same concentration were prepared and no quenching can be observed in the solution phase, indicating that the host and dopant are required to be in close proximity for substantial energy transfer to occur. The observed energy transfer is consistent with a Förster mechanism,[53] though other mechanisms, such as Dexter transfer,[54] cannot be ruled out due to the close proximity of host and guest molecules. A significant feature of the blend nanoparticles is the enlarged energy gap between absorption and fluorescence as compared to the polymers in THF solutions and pure polymer nanoparticles.[21] In addition, nanoparticles with different emission wavelengths can be simultaneously excited by using a single light source, a useful feature for multiplexed fluorescence detection.

Highly efficient energy transfer is evident in the evolution of the fluorescence spectra with increasing dopant concentration. The left side of Figure 3 shows the fluorescence emission spectra of the three types of blend nanoparticles as dopant concentration is increased. As exemplified by the PF/PFPV system, the

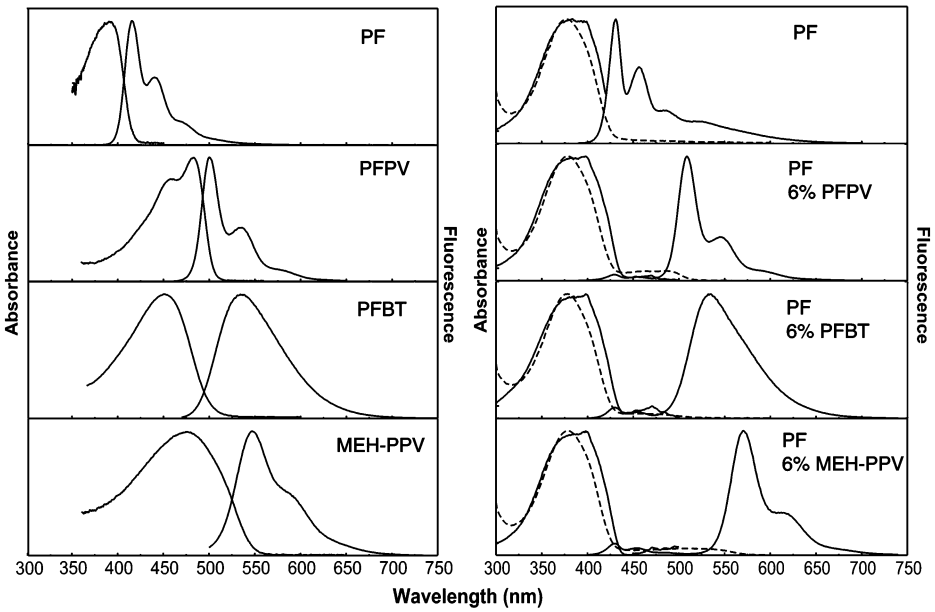

Figure 2. (Left) Normalized absorption and fluorescence emission spectra of conjugated polymers PF, PFPV, PFBT, and MEH−PPV in THF solution. (Right) Normalized absorption (dashed) and fluorescence excitation and emission spectra (solid) of pure PF and polymer blend nanoparticles.

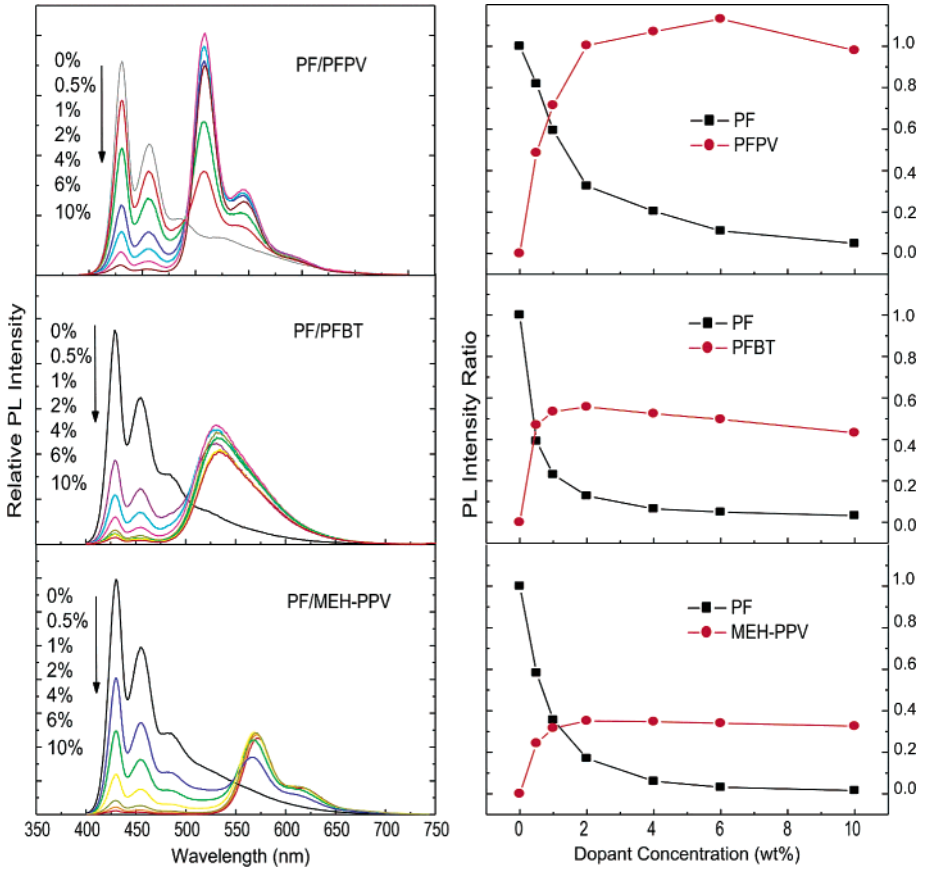

Figure 3. (Left) Concentration-dependent fluorescence spectra of polymer blend nanoparticles under 375 nm excitation. (Right) Fluorescence intensity change of PF host and dopant polymers as a function of dopant concentration in blend nanoparticles. All fluorescence emission intensities were normalized to the 430 nm emission of pure PF nanoparticles.

fluorescence from the PF host decreases with increasing PFPV content, while that from PFPV increases and reaches a maximum around 6 wt %, after which a further increase in dopant concentration causes a slight reduction in fluorescence intensity. Over a concentration range of 2−6%, the PF/PFPV nanoparticles present an intense characteristic emission (510 nm) from PFPV, which is slightly larger than the 430 nm emission from pure (undoped) PF nanoparticles. The other two types of blend nanoparticles show a similar trend in the host fluorescence, but lower dopant fluorescence intensity, consistent with the lower fluorescence quantum yields of PFBT and MEH−PPV as compared to PFPV. In view of the low dopant concentration and rapid nanoparticle formation, together with spectroscopic evidence that indicates an absence of aggregate species, we conclude that the dopant polymer molecules are likely uniformly distributed in the PF host, without significant segregation or

aggregation. In addition, the lack of aggregate features (which are typically associated with reductions in quantum yield) indicates that a higher fluorescence quantum yield can be achieved in the polymer blend system as compared with that of the pure polymer nanoparticles, as discussed below.

3.3. Nanoparticle Energy Transfer Model. The dependence of host polymer fluorescence intensity on the concentration of dopant (quencher) was modeled by using the Stern−Volmer relation, which can be expressed as[53]

$$F_0/F = 1 + K_{SV}[Q] \tag{1}$$

where F_0 and F are fluorescence intensities in the absence and presence of quencher, respectively, K_{SV} is the Stern−Volmer quenching constant, and [Q] is the concentration of the quencher. The quenching constant is obtained from the slope of a linear fit to a plot of F_0/F versus [Q]. However, deviations from the linear relationship can be observed when quenching efficiencies are very high, as observed in the superquenching of conjugated polyelectrolytes by gold nanoparticles.[16] For the polymer blend nanoparticles with PFPV or MEH−PPV as quencher, the F_0/F data deviated substantially from the linear Stern−Volmer relation, while those of PFBT quenchers follow a linear Stern−Volmer behavior over a wide concentration range. If the quencher concentration is expressed as a molecule fraction, the K_{SV} obtained from the plot then represents the number of host molecules quenched by a single quencher. This analysis (Figure 4, solid) indicated that ~65 PF molecules are quenched by a single PFBT molecule, and more than 500 PF molecules are quenched by single molecules of either PFPV or MEH−PPV.

The combination of highly efficient energy transfer and statistical variations in the number of quencher molecules per nanoparticle is likely to cause significant deviations from the Stern−Volmer relationship. Here we introduce a nanoparticle energy transfer model that takes into account the effect of multiple quencher species per nanoparticle and the statistical distribution of quenchers. If we assume that the overall energy transfer rate scales linearly with the number of quenchers, then the host quantum yield is given by the expression

$$\phi = \frac{k_r}{k_r + k_{nr} + nk_{et}} \tag{2}$$

where k_r and k_{nr} are the radiative and nonradiative rates of the host, k_{et} is the energy transfer rate of a single quencher, and n is the number of quenchers present in the nanoparticle. The fraction of nanoparticles with n quenchers per nanoparticle can be described by the Poisson probability distribution function,

$$P(n,\bar{n}) = \frac{(\bar{n})^n}{n!\,\exp(\bar{n})} \tag{3}$$

where $\bar{n}$ is the average number of donor molecules per nanoparticle. Combining this with the above rate expression and introducing a quenching efficiency parameter q given by

$$q = \frac{k_{et}}{k_{et} + k_r + k_{nr}} \tag{4}$$

yields the expression

$$\frac{F}{F_0} = \sum_n \frac{P(n,\bar{n})}{1 + nq/(1-q)} \tag{5}$$

which relates the relative fluorescence intensity (F/F_0) to the quenching efficiency per quencher molecule (q) and the statistical distribution of quencher molecules per nanoparticle. While the model yields results similar to the linear Stern−Volmer model for small values of q, above $q = 0.5$ there are substantial deviations associated with the Poisson statistics. A similar approach, with somewhat different assumptions, was developed by Turro and Yekta for applying fluorescence quenching methods to determine the aggregation number of micelles.[55]

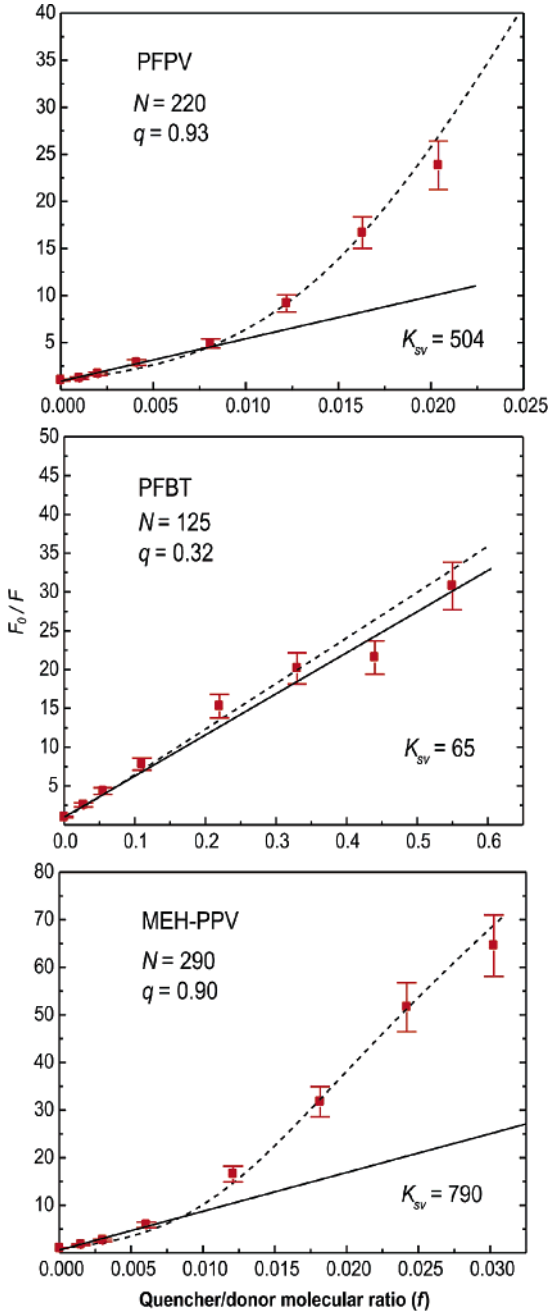

Figure 4. Fluorescence quenching of PF donor versus molar fraction of quenchers in polymer blend nanoparticles. The scattered squares are experimental data, while the black dashed curves are model results given by eq 5. The solid lines represent linear Stern−Volmer plots of PF fluorescence quenched by three quenchers in the low concentration range. The parameters used in the fitting are listed in the figure.

In applying the nanoparticle energy transfer model to the data of Figure 3, it was assumed that $\bar{n} = fN$, where f is the molecular fraction of quenchers (estimated from the dopant weight fraction and the molecular weights of the PF and quencher) and N is the number of donor molecules. The quencher efficiency q and the nanoparticle particle size N were adjusted to obtain the best

fit to the data. Figure 4 shows the experimental (scattered squares) and fit results (dashed lines) for the fluorescence quenching of PF donor by three different quenchers in polymer blend nanoparticles. In each case, the fit is better than that obtained from the Stern−Volmer analysis, particularly at high quencher fractions. For the case of PFBT as quencher, the fit yielded parameters $N = 125$ and $q = 0.32$. $N = 125$ represents the average number of molecules per nanoparticle, which is in good agreement with the value estimated from AFM measurements. $q = 0.32$ indicates that 32% of the fluorescence of a PF nanoparticle would be quenched by a single PFBT molecule, similar to the phenomenon of superquenching observed in nanoparticle assembled dye aggregates.[15,56] The model was also fit to the results obtained with PFPV and MEH−PPV as quenchers. The N parameter obtained from the fit is ∼200 molecules per nanoparticle, corresponding to a particle diameter of ∼30 nm, slightly larger than that obtained from AFM measurements. It is likely that the deviation in N is related to the quencher polydispersity and other factors not taken into account in the model. Interestingly, the large quenching efficiency ($q = \sim 0.9$) obtained for PFPV and MEH−PPV molecules indicates that the fluorescence from a PF nanoparticle consisting of 100−200 molecules could be nearly completely quenched by a single PFPV or MEH−PPV molecule. Considering Förster resonance energy transfer as the dominant mechanism in the quenching process, the difference between the quenching efficiency of PFBT and that of PFPV and MEH−PPV can be attributed to differences in the extinction coefficients. The peak molar extinction coefficients for PFPV, PFBT, and MEH−PPV molecules in THF were determined by absorption measurements to be 5.7×10^7, 4.6×10^5, and 1.5×10^7 M^{-1} cm^{-1}, respectively. Although all the three quenchers show good spectral overlap between their absorptions and the PF fluorescence, the large extinction coefficients of PFPV and MEH−PPV lead to their higher quenching efficiency as compared to PFBT molecules. According to the predictions of the energy transfer model, for quenchers with a relatively low quenching efficiency ($q < 0.5$) the ratio F_0/F depends approximately linearly on the quencher fraction over a wide range, while for highly efficient quenchers, the ratio F_0/F does not have a linear dependence on the quencher fraction. This agrees with our experimental observation that PFBT, the least efficient quencher due to its low molecular absorptivity, closely follows the linear Stern−Volmer relation, while the larger, highly efficient PFPV and MEH−PPV quenchers exhibit substantial deviations from linear Stern−Volmer behavior. On the basis of the success of the nanoparticle energy transfer model in providing quantitative agreement with the spectroscopic results and the simple, intuitive picture it provides for describing the effect of highly efficient quenchers and the statistical variability in the number of quenchers per nanoparticle on the overall energy transfer efficiency, we believe this model will be useful for related systems such as superquenching-based sensors.[14−19]

Both the Stern−Volmer analysis and analysis with the energy transfer model indicate that a single quencher molecule can effectively quench the fluorescence of hundreds of host molecules. In terms of a quenching volume or radius, this yields a result similar to those observed for doped fluorescent molecular crystals[26,57] and quenching by charge carriers in MEH−PPV films.[58] If the quenching were described by one-step Förster energy transfer, the number of PF molecules that can be quenched by a single PFBT molecule would be determined by the Förster radius, which is in the range of 5−10 nm, not sufficient to account for the large quenching volumes observed. Because of the substantial spectral overlap between the absorption and emission of the PF donor, there is also the possibility of multiple energy transfer between molecules of PF, a process characterized by an energy diffusion length, typically on the order of 5−15 nm for conjugated polymers.[59] Thus we conclude that the large quenching efficiency is likely due to a combination of energy diffusion and host−guest energy transfer that can effectively result in the quenching of hundreds of host polymers by a single quencher. On the basis of these considerations and the experimental evidence of relatively long-range energy transfer, it appears possible to construct probes based on energy transfer quenching using ∼10−20 nm diameter conjugated polymer nanoparticles.[37]

We previously observed that the conjugated polymer nanoparticles suffered from a reduction in fluorescence quantum yield as compared with the polymers in organic solvent.[21] Similar reductions in fluorescence quantum yield are typically observed for thin films of conjugated polymer (as compared to solution) and are attributed to interactions between polymer chain segments which can result in the formation of red-shifted, weakly fluorescent aggregate species. A fluorescence quantum yield of 10% was determined for pure PFPV nanoparticles, as described in our previous report.[21] However, for the case of blended nanoparticles, the polymer acceptors are uniformly distributed, with no discernible aggregate features in the fluorescence spectrum. If energy transfer to aggregate species is the primary loss mechanism, then one might expect that a higher quantum yield could be achieved in the PF/PFPV blend nanoparticles as compared to pure PFPV nanoparticles. Furthermore, nearly all of the excitation energy absorbed by hundreds of PF molecules is transferred to the PFPV, resulting in a large increase in absorptivity and therefore large improvements in fluorescence brightness as compared to smaller particles consisting of single polymer molecules. A fluorescence quantum yield of 14% and a peak extinction coefficient of 1.5×10^9 M^{-1} cm^{-1} (assuming 200 molecules per nanoparticle) were determined for PF nanoparticles doped with PFPV (6 wt %) suspended in water, using a solution of Coumarin 1 in ethanol as a standard.[60] The fluorescence brightness is defined as the product of the extinction coefficient and the quantum yield. The calculated fluorescence brightness of PF/PFPV blend nanoparticles is more than 2000 times higher than that of rhodamine 6G. For comparison, the fluorescence brightness of quantum dots has been reported to be in the range of 20 times that of rhodamine dyes,[2] and dye-loaded silica particles of ∼30 nm in diameter have a reported brightness equivalent to approximately 100 rhodamine molecules.[7] The high brightness of the conjugated polymer blend nanoparticles compares favorably with that of quantum dots and dye-loaded silica colloids. While thorough investigations of photostability of the particles have not yet been completed, qualitative observations indicate that suspensions of the nanoparticles fade at rates substantially lower than those of fluorescein solutions of similar absorptivity. We previously demonstrated that encapsulating small conjugated polymer nanoparticles with silica can improve photostability.[21] The high brightness, combined with the improved photostability, is very promising for biological labeling and sensing applications.

4. Conclusions

PF nanoparticles doped with PFPV, PFBT, and MEH−PPV, respectively, were prepared by a reprecipitation method. Salient features of the nanoparticles include their high fluorescence brightness and suitability for fluorescence multiplexing applica-

tions. In some cases, the dependence of nanoparticle fluorescence on composition was found to deviate substantially from the Stern−Volmer relation. A nanoparticle energy transfer model was developed that takes into account statistical variability in nanoparticle composition, and provides excellent agreement with experimental results, particularly for the dopants with high quenching efficiencies. Analyses by both Stern−Volmer relation and the nanoparticle energy transfer model reveal highly efficient energy transfer between the host and the guest molecules. Both models indicate that approximately 100 or more host molecules are quenched by a single dopant molecule. This result is interpreted as evidence of long-range (>10 nm) energy transport by multiple energy transfer. The fluorescence spectroscopy of the blended nanoparticles indicates a lack of aggregate features and improvements in fluorescence quantum yield. On the basis of the molar absorptivity and quantum yield, the fluorescence brightness of the blend nanoparticles is estimated to be ∼100 times larger than that of quantum dots, and 20 times higher than that of dye-loaded silica spheres of similar dimensions.

Acknowledgment. The authors gratefully acknowledge financial support from Clemson University, NSF-EPSCoR, and an NSF-CAREER Award. We would also like to thank Dvora Perahia for her assistance in AFM measurements.

References and Notes

(1) Bruchez, M.; Moronne, M.; Gin, P.; Weiss, S.; Alivisatos, A. P. *Science* **1998**, *281*, 2013.
(2) Chan, W. C. W.; Nie, S. M. *Science* **1998**, *281*, 2016.
(3) Larson, D. R.; Zipfel, W. R.; Williams, R. M.; Clark, S. W.; Bruchez, M. P.; Wise, F. W.; Webb, W. W. *Science* **2003**, *300*, 1434.
(4) Zhao, X. J.; Hilliard, L. R.; Mechery, S. J.; Wang, Y. P.; Bagwe, R. P.; Jin, S. G.; Tan, W. H. *Proc. Natl. Acad. Sci. U.S.A.* **2004**, *101*, 15027.
(5) Alivisatos, A. P.; Gu, W. W.; Larabell, C. *Annu. Rev. Biomed. Eng.* **2005**, *7*, 55.
(6) Alivisatos, P. *Nat. Biotechnol.* **2004**, *22*, 47.
(7) Ow, H.; Larson, D. R.; Srivastava, M.; Baird, B. A.; Webb, W. W.; Wiesner, U. *Nano Lett.* **2005**, *5*, 113.
(8) Michalet, X.; Pinaud, F. F.; Bentolila, L. A.; Tsay, J. M.; Doose, S.; Li, J. J.; Sundaresan, G.; Wu, A. M.; Gambhir, S. S.; Weiss, S. *Science* **2005**, *307*, 538.
(9) Wang, L.; Yang, C. Y.; Tan, W. H. *Nano Lett.* **2005**, *5*, 37.
(10) Halls, J. J. M.; Walsh, C. A.; Greenham, N. C.; Marseglia, E. A.; Friend, R. H.; Moratti, S. C.; Holmes, A. B. *Nature* **1995**, *376*, 498.
(11) Friend, R. H.; Gymer, R. W.; Holmes, A. B.; Burroughes, J. H.; Marks, R. N.; Taliani, C.; Bradley, D. D. C.; Dos Santos, D. A.; Bredas, J. L.; Loglund, M.; Salaneck, W. R. *Nature* **1999**, *397*, 121.
(12) Pei, Q.; Yu, G.; Zhang, C.; Yang, Y.; Heeger, A. *Science* **1995**, *269*, 1086.
(13) Yu, G.; Gao, J.; Hummelen, J. C.; Wudl, F.; Heeger, A. J. *Science* **1995**, *270*, 1789.
(14) Chen, L.; McBranch, D. W.; Wang, H. L.; Helgeson, R.; Wudl, F.; Whitten, D. G. *Proc. Natl. Acad. Sci. U.S.A.* **1999**, *96*, 12287.
(15) Jones, R. M.; Lu, L. D.; Helgeson, R.; Bergstedt, T. S.; McBranch, D. W.; Whitten, D. G. *Proc. Natl. Acad. Sci. U.S.A.* **2001**, *98*, 14769.
(16) Fan, C. H.; Wang, S.; Hong, J. W.; Bazan, G. C.; Plaxco, K. W.; Heeger, A. J. *Proc. Natl. Acad. Sci. U.S.A.* **2003**, *100*, 6297.
(17) Xu, Q. H.; Gaylord, B. S.; Wang, S.; Bazan, G. C.; Moses, D.; Heeger, A. J. *Proc. Natl. Acad. Sci. U.S.A.* **2004**, *101*, 11634.
(18) Kumaraswamy, S.; Bergstedt, T.; Shi, X. B.; Rininsland, F.; Kushon, S.; Xia, W. S.; Ley, K.; Achyuthan, K.; McBranch, D.; Whitten, D. *Proc. Natl. Acad. Sci. U.S.A.* **2004**, *101*, 7511.
(19) Pinto, M. R.; Schanze, K. S. *Proc. Natl. Acad. Sci. U.S.A.* **2004**, *101*, 7505.
(20) Kim, I. B.; Dunkhorst, A.; Bunz, U. H. F. *Langmuir* **2005**, *21*, 7985.
(21) Wu, C.; Szymanski, C.; McNeill, J. *Langmuir* **2006**, *22*, 2956.
(22) Szymanski, C.; Wu, C.; Hooper, J.; Salazar, M. A.; Perdomo, A.; Dukes, A.; McNeill, J. D. *J. Phys. Chem. B* **2005**, *109*, 8543.
(23) Powell, R. C. *Phys. Rev. B* **1970**, *2*, 2090.
(24) Li, C. S.; Kopelman, R. *Macromolecules* **1990**, *23*, 2223.
(25) Li, C. S.; Kopelman, R. *J. Phys. Chem.* **1990**, *94*, 2135.
(26) McNeill, J. D.; Kim, D. Y.; Barbara, P. F. *J. Phys. Chem. B* **2004**, *108*, 11368.
(27) Shen, Y. Z.; Friend, C. S.; Jiang, Y.; Jakubczyk, D.; Swiatkiewicz, J.; Prasad, P. N. *J. Phys. Chem. B* **2000**, *104*, 7577.
(28) Liddell, P. A.; Kodis, G.; Andreasson, J.; de la Garza, L.; Bandyopadhyay, S.; Mitchell, R. H.; Moore, T. A.; Moore, A. L.; Gust, D. *J. Am. Chem. Soc.* **2004**, *126*, 4803.
(29) Lee, T. H.; Kumar, P.; Mehta, A.; Xu, K. W.; Dickson, R. M.; Barnes, M. D. *Appl. Phys. Lett.* **2004**, *85*, 100.
(30) Kumar, P.; Lee, T. H.; Mehta, A.; Sumpter, B. G.; Dickson, R. M.; Barnes, M. D. *J. Am. Chem. Soc.* **2004**, *126*, 3376.
(31) Hu, D. H.; Yu, J.; Barbara, P. F. *J. Am. Chem. Soc.* **1999**, *121*, 6936.
(32) Yu, Z. H.; Barbara, P. F. *J. Phys. Chem. B* **2004**, *108*, 11321.
(33) Barbara, P. F.; Gesquiere, A. J.; Park, S. J.; Lee, Y. J. *Acc. Chem. Res.* **2005**, *38*, 602.
(34) Jonkheijm, P.; Miura, A.; Zdanowska, M.; Hoeben, F. J. M.; De Feyter, S.; Schenning, A. P. H. J.; De Schryver, F. C.; Meijer, E. W. *Angew. Chem., Int. Ed.* **2004**, *43*, 74.
(35) Spano, F. C. *J. Chem. Phys.* **2005**, *122*, 234701.
(36) Medintz, I. L.; Uyeda, H. T.; Goldman, E. R.; Mattoussi, H. *Nat. Mater.* **2005**, *4*, 435.
(37) Medintz, I. L.; Clapp, A. R.; Mattoussi, H.; Goldman, E. R.; Fisher, B.; Mauro, J. M. *Nat. Mater.* **2003**, *2*, 630.
(38) Clapp, A. R.; Medintz, I. L.; Fisher, B. R.; Anderson, G. P.; Mattoussi, H. *J. Am. Chem. Soc.* **2005**, *127*, 1242.
(39) Lu, L. D.; Helgeson, R.; Jones, R. M.; McBranch, D.; Whitten, D. *J. Am. Chem. Soc.* **2002**, *124*, 483.
(40) Waner, M. J.; Gilchrist, M.; Schindler, M.; Dantus, M. *J. Phys. Chem. B* **1998**, *102*, 1649.
(41) Yang, Z. Q.; Huck, W. T. S.; Clarke, S. M.; Tajbakhsh, A. R.; Terentjev, E. M. *Nat. Mater.* **2005**, *4*, 486.
(42) Chen, L. C.; Roman, L. S.; Johansson, D. M.; Svensson, M.; Andersson, M. R.; Janssen, R. A. J.; Inganas, O. *Adv. Mater.* **2000**, *12*, 1110.
(43) Xu, Q. F.; Duong, H. M.; Wudl, F.; Yang, Y. *Appl. Phys. Lett.* **2004**, *85*, 3357.
(44) Gong, X.; Wang, S.; Moses, D.; Bazan, G. C.; Heeger, A. J. *Adv. Mater.* **2005**, *17*, 2053.
(45) Gong, X.; Ostrowski, J. C.; Bazan, G. C.; Moses, D.; Heeger, A. J.; Liu, M. S.; Jen, A. K. Y. *Adv. Mater.* **2003**, *15*, 45.
(46) Kietzke, T.; Neher, D.; Landfester, K.; Montenegro, R.; Guntner, R.; Scherf, U. *Nat. Mater.* **2003**, *2*, 408.
(47) Babel, A.; Li, D.; Xia, Y. N.; Jenekhe, S. A. *Macromolecules* **2005**, *38*, 4705.
(48) Collison, C. J.; Rothberg, L. J.; Treemaneekarn, V.; Li, Y. *Macromolecules* **2001**, *34*, 2346.
(49) Nguyen, T.-Q.; Martini, I. B.; Liu, J.; Schwartz, B. J. *J. Phys. Chem. B* **2000**, *104*, 237.
(50) Padmanaban, G.; Ramakrishnan, S. *J. Am. Chem. Soc.* **2000**, *122*, 2244.
(51) Scherf, U.; List, E. J. W. *Adv. Mater.* **2002**, *14*, 477.
(52) Yang, X. H.; Jaiser, F.; Neher, D.; Lawson, P. V.; Bredas, J. L.; Zojer, E.; Guntner, R.; de Freitas, P. S.; Forster, M.; Scherf, U. *Adv. Funct. Mater.* **2004**, *14*, 1097.
(53) Lakowicz, J. R. *Principles of Fluorescence Spectroscopy*; Plenum Press: New York, 1999.
(54) Dexter, D. L. *J. Chem. Phys.* **1953**, *21*, 836.
(55) Turro, N. J.; Yekta, A. *J. Am. Chem. Soc.* **1978**, *100*, 5951
(56) Lu, L. D.; Jones, R. M.; McBranch, D.; Whitten, D. *Langmuir* **2002**, *18*, 7706.
(57) Campillo, A. J.; Shapiro, S. L.; Swenberg, C. E. *Chem. Phys. Lett.* **1977**, *52*, 11.
(58) McNeill, J. D.; Barbara, P. F. *J. Phys. Chem. B* **2002**, *106*, 4632.
(59) Halls, J. J. M.; Pichler, K.; Moratti, S. C.; Holmes, A. B. *Appl. Phys. Lett.* **1996**, *68*, 3120.
(60) Jones, G.; Jackson, W. R.; Choi, C.; Bergmark, W. R. *J. Phys. Chem.* **1985**, *89*, 294.